

GridCLIP: One-Stage Object Detection by Grid-Level CLIP Representation Learning

Jiayi Lin
Queen Mary University of London
jiayi.lin@qmul.ac.uk

Shaogang Gong
Queen Mary University of London
s.gong@qmul.ac.uk

Abstract

A vision-language foundation model pretrained on very large-scale image-text paired data has the potential to provide generalizable knowledge representation for downstream visual recognition and detection tasks, especially on supplementing the undersampled categories in downstream model training. Recent studies utilizing CLIP for object detection have shown that a two-stage detector design typically outperforms a one-stage detector, while requiring more expensive training resources and longer inference time. In this work, we propose a one-stage detector GridCLIP that narrows its performance gap to those of two-stage detectors, with approximately $43\times$ and $5\times$ faster than its two-stage counterpart (ViLD) in the training and test process respectively. GridCLIP learns grid-level representations to adapt to the intrinsic principle of one-stage detection learning by expanding the conventional CLIP image-text holistic mapping to a more fine-grained, grid-text alignment. This differs from the region-text mapping in two-stage detectors that apply CLIP directly by treating regions as images. Specifically, GridCLIP performs Grid-level Alignment to adapt the CLIP image-level representations to grid-level representations by aligning to CLIP category representations to learn the annotated (especially frequent) categories. To learn generalizable visual representations of broader categories, especially undersampled ones, we perform Image-level Alignment during training to propagate broad pre-learned categories in the CLIP image encoder from the image-level to the grid-level representations. Experiments show that the learned CLIP-based grid-level representations boost the performance of undersampled (infrequent and novel) categories, reaching comparable detection performance on the LVIS benchmark.

1. Introduction

Simultaneous multi-category object detection aims to both recognize (classify) and detect (locate) all instances

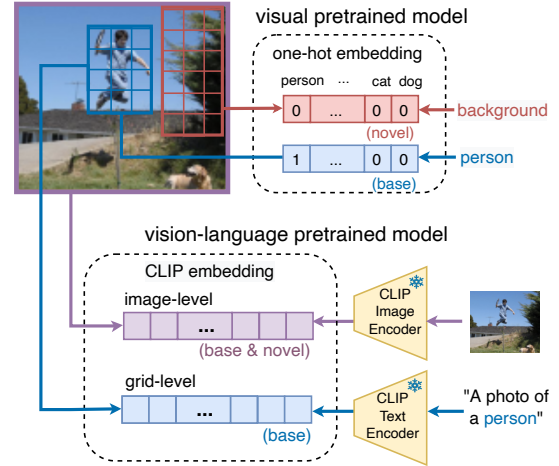


Figure 1. Comparison of approaches to applying visual pretrained and vision-language pretrained models (GridCLIP as an example) to one-stage detectors. The visual pretrained model is commonly used for extracting grid-level image representations (also called feature maps) which are aligned to the manual one-hot embeddings, so only base categories can be learned (top). While in a vision-language pretrained model, images are encoded into high-dimension embeddings, which can be aligned to the text embeddings of base categories as well as the whole image embedding of both base and novel categories (bottom).

of given categories in an image. A significant challenge in training a good detector is the cost of labeling a large-scale dataset on a broad range of object categories with balanced data distributions. Existing detection datasets are often imbalanced with a long-tail distribution across categories [24] where some object categories have only a few or zero training sample(s). To deal with these undersampled categories, few-shot and zero-shot learning have been explored, but they are inherently weaker models when compared to a fully supervised learning based model.

Elsewhere, Self-Supervised Learning (SSL) has received increasing research interest for exploring widely available unlabelled data. Self-supervised pretraining followed by supervised fine-tuning for constructing a detector has been

proposed recently [32, 30]. An example is Open Vocabulary Object Detection (OVOD) [34], which pretrains a model on image-caption pairs containing a substantial amount of broad categories, followed by fine-tuning the model on a detection specific dataset of only a few base categories. For the pretraining stage that supplements knowledge for undersampled categories, Vision-Language pretrained Models (VLMs) are widely adopted. As one of the most widely adopted VLMs, CLIP [21] is pretrained on a dataset of 400 million image-text pairs with a vocabulary of over 49,000 words, providing generalizable visual embeddings of broad categories that helps supplement the undersampled categories in a detection dataset.

Recent approaches have been exploring the CLIP-based representation for object detection, mostly for Open-Vocabulary Object Detection (OVOD) [9, 41]. These detectors can be broadly considered as two-stage detectors [9, 38, 5, 7, 14] and one-stage detectors [31, 22, 20]. Although a one-stage detector is inherently simpler and less costly to compute, it suffers from poorer performance than that of a two-stage detector using CLIP [20]. In this work, we propose a CLIP-based one-stage detector GridLCIP that narrows the performance gap from typical two-stage detectors, while requires a much shorter training time ($43\times$ less compared to ViLD [9]) and test time ($5\times$ faster).

Specifically, we learn grid-level representations of images that can be further used for classification, since an object in one-stage detectors is noted by the category of a grid (a pixel in a feature map) and its corresponding bounding box. Therefore, we expand the conventional CLIP image-text holistic mapping to grid-text mapping, namely *Grid-level Alignment*. Although some other one-stage detectors [20] also share similar spirits, they align the image embeddings trained from supervised or visual data only self-supervised learning methods (rather than CLIP-like visual-language pretrained models) to align with CLIP text embeddings. While we directly adapt the CLIP image embeddings to generate grid-level embeddings, which directly benefits from the generalizability of the CLIP image encoder and is intrinsically more consistent with CLIP text embeddings. However, similar to DenseCLIP [22] which can only perform close-set detection, grid-level alignment is only performed on the base categories without the scope to learn knowledge of novel (unseen) categories for open-set detection.

To further exploit CLIP to learn representation for novel categories, some approaches [41, 20, 8, 7] used extra image-caption or labeled datasets like CC3M [25] or ImageNet-21K [3], making the training process complicated and resource-consuming. In this work, we want to explore CLIP directly without the need of extra image-caption and/or labelled training data in order to learn novel categories by applying knowledge distillation on CLIP. As revealed in Hi-

erKD [20], the gap between one-stage and two-stage detectors is that the knowledge distillation on two-stage detectors happen on image regions of both base and novel categories [9, 41] given by a separate pretrained region proposal network (RPN), hence two-stage, while the one-stage detectors mainly only use base categories for knowledge distillation [31]. Therefore, HierKD aligns the text embedding of the caption to its paired image embedding, and further uses an attention layer for adapting the gap between captions and images. However, HierKD requires the training images to have paired captions in addition to detection annotations, making it unscalable to training on other detection datasets for more general detection tasks. To avoid all these additional requirements on model training, we propose to use visual-to-visual alignment instead of caption-to-visual alignment. This is designed to learn the visual embeddings of both base and novel categories without the need for further adaptation. We call it *Image-level Alignment*. Specifically, we align the image-level embeddings with the one that is generated by a fixed CLIP image encoder (teacher). Since the feature extractor of image-level embeddings and grid-level embeddings are mainly shared, the grid-level embeddings can implicitly obtain knowledge of undersampled categories from the teacher. In this way, we implicitly train the grid-level embeddings to align to both base and novel categories in CLIP space.

Overall, we propose a one-stage detector GridCLIP, which exploits CLIP to supplement the knowledge of undersampled categories in downstream detection datasets by simultaneously applying grid-level and image-level alignments. Our contributions are: (1) We exploit CLIP to supplement the missing knowledge of undersampled object detection categories in training a one-stage detector, mitigating the poor performance due to the long-tail data distribution in most existing detection training data. (2) We propose a simple yet effective visual-to-visual knowledge distillation method for learning novel categories in constructing a one-stage CLIP-based detector, providing 2.4 AP gains on novel categories compared to the baseline. (3) GridCLIP is capable of handling Open-Vocabulary Object Detection with considerable scalability and generalizability, reaching the comparable performance to two-stage detectors in Open-Vocabulary Object Detection with much higher training and inference speed, without using extra pretraining processes or additional fine-tuning datasets.

2. Related Works

Vision-Language Pretrained Model (VLM). Visual-only pretrained model has dominated the pretraining process for several years until VLMs have appeared. In comparison, Vision-Language Pretrained Models (VLMs) are able to align more visual concepts out of manual predefined categories to natural language, extending the generality of the

model. Recently, a considerable number of vision-language pretrained models [21, 26, 13, 33] emerge, training from large-scale image-text data in an unsupervised way. These models usually have both image and text encoders to generate corresponding features that can be aligned in a cross-modality representational space for corresponding image-text matching. Utilizing these alignment spaces helps zero-shot transfer to a wide range of downstream visual recognition tasks, such as object detection [12, 5, 7], segmentation [39, 19], image retrieval [36, 15]. As one widely-used instance, CLIP [21] is trained on 400 million image-text pairs through a contrastive objective, which extends significantly the generalizability and usability of the learned image embeddings to align to broad categories, showing competitive performance with its fully supervised counterparts. CLIP is widely applied both in downstream tasks oriented pretraining [38, 16] and in fine-tuning for downstream tasks [9, 22].

Object Detection using VLM. OVR-CNN [34] is the first to utilize natural language (captions) for object detection. While recent detectors apply large-scale image-text datasets to learn generalizable image representations. Some VLMs like GLIP [16] and DetCLIP [35] utilize large-scale annotation datasets in addition to image-text pairs for pertaining, which requires relatively high annotation cost. While we focus on utilizing unsupervised VLMs like CLIP and learn from annotation datasets of a limited number of categories to transfer to broader categories.

To learn knowledge of base categories, most detectors [9, 41] replace the classifiers of their detection heads with VLM text embeddings. Recent detectors mainly improve the learning in two aspects: learning better text embeddings of categories and extracting image embeddings to align with these text embeddings. (1) For generating better text embeddings, also called *Prompt Learning*, current approaches can be roughly classified as template-based and learnable prompting. The template-based one uses fixed incomplete sentences that can accept labels to build complete sentences [9, 20, 38], while the learnable prompting methods concatenate learnable parameters with category labels as the input, where the prompt is implicitly learned during fine-tuning [40, 5, 7]. GridCLIP uses template-based prompting as in the original CLIP and some OVOD detectors [9, 20, 38] for simplicity and scalability. (2) For extracting image embeddings to align with text embeddings, two-stage detectors [23, 27, 9, 41, 5, 38] use the embedding of cropped object bounding-box proposals. However, they need to train a region proposal network first and require multiple inferences of the CLIP image encoder to compute the visual embedding for each region, which is relatively inefficient. In comparison, a one-stage detector [17, 28, 22] aligns parts in an image represented by grid-level embeddings. DenseCLIP [22] adapt it as aligning grid-level image

features with text, while can only perform under close-set settings. While HierKD [20] performs image-level, region-level and grid-level alignment to CLIP, which however requires the match captions with the detection dataset, limiting its deployment to other downstream detection datasets. Our method uses grid-level alignment for efficiency while preserving the original alignment space of CLIP to gain better generalization ability, without requiring extra datasets.

To learn knowledge of novel categories, some approaches [41, 20, 8, 7] use extract knowledge from external datasets extra image-caption or labeled datasets like CC3M [25] or ImageNet-21K [3], making the training process complicated and resource-consuming. While we argue that CLIP has been trained over a broad vocabulary and has the ability to provide visual embeddings of various categories. Therefore, we explore the original CLIP representation space to learn novel categories by applying knowledge distillation on CLIP as in ViLD [9].

3. Approach

The overall model design of GridCLIP is shown in Figure 2. We first introduce the strategy of adopting the CLIP embeddings for a detection task, and then present the approach to mapping simultaneously the CLIP representation by both grid-level and image-level alignments based on a one-stage detector FCOS [28].

3.1. Adapting CLIP for Detection

CLIP consists of an image encoder (ResNet [11] or ViT [4]) and a text encoder (Transformer [29]), which together form the alignment space of visual and language embeddings. However, as the image embedding in CLIP is a high-dimensional feature vector of an entire image instead of a spatial region or pixels, and the text embedding is encoded from a sentence instead of a single category label in detection, further adaptation for the detection task is needed.

Generating Image Embedding. The original CLIP image feature \bar{z} is a single high-dimensional feature vector representing an entire image without spatial information. To get the grid-level feature z , inspired by DenseCLIP [22], we use the other feature from the last layer of the CLIP image encoder. Specifically, taking the ResNet50 encoder as an example, the final output feature in the 5-th stage $C_5 \in \mathbf{R}^{H_5 \times W_5 \times D_5}$ is first performed global average pooling to get the image-level feature $\bar{C}_5 \in \mathbf{R}^{1 \times 1 \times D_5}$, where H_5, W_5, D_5 are the height, width and number of channels of the feature in the 5-th stage of the ResNet50. Then the concatenated features $[\bar{C}_5, C_5]$ are fed into a Multi-Head Self-Attention (MHSA) layer [29] as follows,

$$[\bar{z}, z] = \text{MHSA}([\bar{C}_5, C_5]). \quad (1)$$

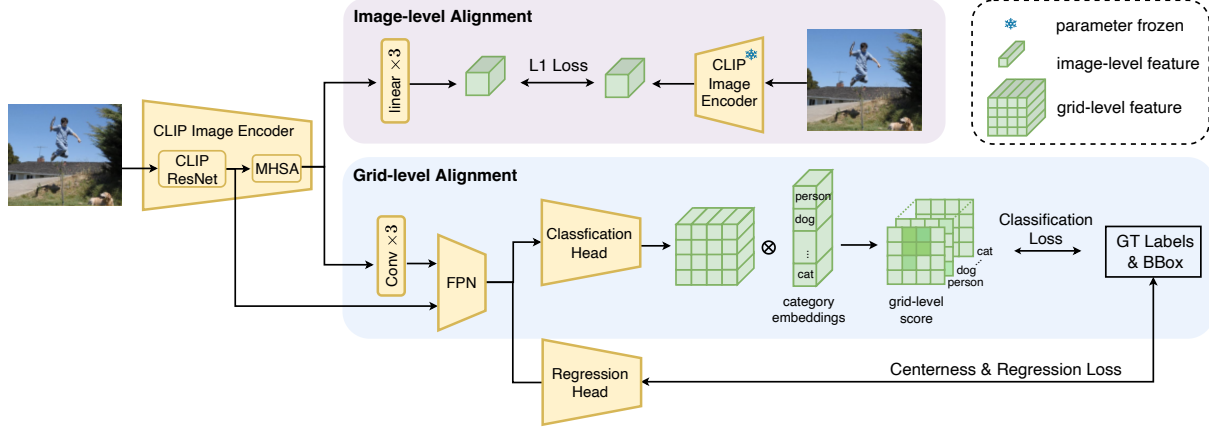


Figure 2. The pipeline of our proposed GridCLIP. GridCLIP aligns to the CLIP representation in both image and grid levels. In image-level alignment, the image-level feature is aligned to the feature generated by a fixed CLIP image encoder. In grid-level alignment, the grid-level feature is aligned to the classification target generated from the ground truth labels and bounding boxes following the detector FCOS [28]. Note that the grid-level alignment is performed in multiple scales, while only one scale is presented here for simplicity.

In CLIP, the output with spatial information z is dumped and \bar{z} is used to match with the text embedding. However, as illustrated in DenseCLIP, since the MHSA is symmetric to each input element, z may behave similarly to \bar{z} , which aligns well with the text embedding. Therefore, we adopt both z and \bar{z} to generate our grid-level and image-level embeddings respectively with a few adaptation layers.

From Label to Text Embedding. In the original CLIP, to create a dataset classifier from label text, a set of template-based prompts like “a photo of a $\{object\}$.” are applied, where $object$ is any of the target category names. Then the multiple prompts for a single label are aggregated. Although there are several learnable prompting methods for CLIP [40] that fine-tune with the downstream tasks, We follow the template-based one for simplicity and scalability. We use one template-based variant in ViLD [9] designed for object detection. Here we note the final text embeddings of the categories in the target dataset (base categories) as $\{T_k\}_{k=1}^K$, where K is the number of category.

3.2. Grid-level Alignment

Generating Grid-level Image Embedding. Taking ResNet50 encoder as an example, in FCOS [28], the output feature map C_3, C_4, C_5 of ResNet50 are inputted into FPN, producing 5 multi-scale image feature maps $\{P_i\}_{i=3}^7$. In FPN, C_5 is fused with C_3, C_4 to produce P_3, P_4 as well as serves as the input of P_6, P_7 . Therefore, we fuse z' into C_5 to spread the image embeddings suitable for the text alignment to different scale image feature maps.

To be specific, we first apply three consecutive 3×3 convolutional layers with ReLU activation function to adapt the MHSA grid-level output feature z , reducing the number of channels from 1024 to 256 to generate z' , and concatenate it with C_5 . Then the concatenated feature $[z', C_5]$ replaces

C_5 and is fed into the FPN with a little modification in the input channel number. In this way, the FPN is able to produce the multi-scale feature maps $\{P_i\}_{i=3}^7$ inheriting from the CLIP image embeddings that can be aligned to the text embedding as formulated below,

$$\{P_i\}_{i=3}^7 = \text{FPN}(C_3, C_4, [z', C_5]). \quad (2)$$

The FPN output feature $\{P_i\}_{i=3}^7$ are then used to generate the final multi-scale grid-level features $\{G_i\}_{i=3}^7$ by going through the FCOS classification head. In the original FCOS, the classification head contains 5 convolutional layers and the last layer outputs the features with the channel number equal to the category number. While in GridCLIP, We instead modify the output channel to be equal to the dimension of the CLIP text embeddings, to generate $\{G_i\}_{i=3}^7$. Then for each scale, the output feature map calculates the cosine similarities with each text embedding (each category) in pixel level corresponding to grids in the original image, to produce the multi-scale grid-level score with the Sigmoid activation function. For any grid (pixel) j in the i -th scale grid-level feature $G_i(j)$, the matching score over all categories can be formulated as below,

$$S_i(j) = \left\{ \frac{G_i(j) \cdot T_k}{\|G_i(j)\|_2 \|T_k\|_2} \right\}_{k=1}^K. \quad (3)$$

Finally, the grid-level score $\{S_i\}_{i=3}^7$ is treated as the original classification output and aligned to the ground-truth target $\{Target_i\}_{i=3}^7$ using Focal Loss [17] as in the original FCOS.

3.3. Image-level Alignment

With grid-level alignment, the image grids of the base categories are mapped to the CLIP alignment space, by

aligning their embeddings to the corresponding text embeddings $\{T_k\}_{k=1}^K$. While for grids of novel categories, there are no corresponding text embeddings to align to, which can only learn their embeddings by minimizing their similarity to any of $\{T_k\}_{k=1}^K$ during training. However, since the embeddings of different novel categories can have different similarities to each base category, simply minimizing the similarities between the base and novel categories is not consistent with the CLIP representation space which presents a generalizable knowledge representation. Therefore, ignoring the alignment of novel categories may limit the ability to encode a wide range of novel visual concepts, which harms the generalization ability of the model.

In practice, inspired by ViLD [9], we align the image-level embedding \bar{z} to the embedding \bar{z}_{CLIP} produced by a fixed CLIP image encoder, so that the regions of novel categories in an image can also be projected to the CLIP alignment space. Different from ViLD that aligns the embedding of several proposed regions in an image provided by a separate region proposal network (RPN), hence two-stage, which is the source of significant extra computational costs due to its requirement for multiple inferences of the image encoder for each object proposal, we directly align the embedding of the whole image \bar{z}' without the need for multiple passes. Specifically, similar to grid-level alignment, we generate the image-level embedding \bar{z}' from \bar{z} going through three consecutive linear layers with the ReLU activation function. Then we maximize the L_1 similarity between \bar{z} and \bar{z}_{CLIP} , the reverse of which is the image-level alignment loss L_{image} . As for the fixed CLIP image encoder, we evaluate different published versions of pre-trained models and choose the ViT-B/32 version for alignment. Note that image-level alignment is only performed during the training phase.

Finally, the total loss for training GridCLIP end-to-end is,

$$L = w_{\text{grid}}L_{\text{grid}} + w_{\text{image}}L_{\text{image}} + L_{\text{R}} + L_{\text{C}}, \quad (4)$$

which includes the loss of two alignments as well as the original loss in the one-stage detector FCOS: Regression loss L_{R} for bounding boxes and centerness loss L_{C} indicating the distance of a pixel to the center of the bounding box.

4. Experiments

4.1. Implementational Details

GridCLIP uses the one-stage detector FCOS [28] as the detector, which can be replaced by other one-stage detectors like RetinaNet [17] or ATSS [37]. The backbone uses the RN50 pretrained CLIP image encoder, which has two more convolutional layers than the original ResNet50 [11] in the stem module and a Multi-Head Self-Attention (MHSA)

layer performing on the output of the 5th stage. The adapting layers performed on the output features of MHSA use the embedding dimension of 256. For image-level alignment, GridCLIP uses the ViT-B/32 version of CLIP. The weights of the two alignment losses are: $w_{\text{grid}}=1$, $w_{\text{image}}=10$. Our implementation is based on the MMDetection framework [2].

We conduct experiments on the detection benchmark LVIS v1.0 [10]. LVIS v1.0 is a long-tail detection dataset containing 1203 categories. The categories are divided into three parts by how many images they appear in: rare (1-10), common (11-100), and frequent (>100), respectively including 337, 461 and 405 categories, with corresponding metrics AP_r , AP_c and AP_f . Following the ViLD [9], we use frequent and common categories as the base categories and rare categories as the novel categories for open-set detection. For close-set detection, we use the common and frequent categories. When comparing with other SOTA approaches, we adopt multi-scale training similar to ViLD and random cropping augmentation. For the training process, GridCLIP is trained for a $2 \times (24 \text{ LVIS epochs})$ schedule with a batch size of 16. During the inference stage, the maximum number of detection objects per image is 300, and the threshold of the classification score is set to 0.05. The IOU threshold of NMS is 0.5. Refer to the supplementary materials for more details.

4.2. Comparison with the State-of-the-Art

We compare GridCLIP on the LVIS v1.0 validation set with other methods with comparable backbone, including ViLD [9], RegionCLIP [38], Detic [41], DetPro [5] and PromptDet [7] in Table 1. These methods use template-based prompts, except that DetPro [5] and PromptDet [7] use learnable prompts. Also, we do not compare to methods like GLIP [16] and DetCLIP [35] which use large-scale annotation data, since we focus on utilizing limited annotation data for the detection of broader categories.

Performance Comparison. A totally fair comparison is not realistic, since external datasets or learnable prompts are widely used in most OVOD methods. Therefore, we find it relatively fair to compare GridCLIP with ViLD [9] which only utilizes the knowledge of CLIP and the detection dataset without learnable prompts. We observe that GridCLIP surpasses ViLD in overall AP by 0.8. As a one-stage detector, GridCLIP closes the gap to the two-stage detector ViLD in novel categories to 1.3 AP_r , while the current SOTA one-stage detector HierKD is still 8.2 AP behind ViLD on the COCO validation dataset. Furthermore, GridCLIP outperforms ViLD by 1.5 AP_c and 0.9 AP_f . Besides ViT-B/32, we also use the RN50 \times 64 version (the largest model of CLIP under ResNet architecture) of CLIP for image-level alignment to explore the upper bound of the ResNet version. We observe that the RN50 \times 64 version

Table 1. Comparison with different object detectors on LVIS v1.0 [10] with open-set settings. Multi-scale training is used. “CLIP on cropped regions” directly applies CLIP to classify cropped region proposals. Except for GridCLIP, all detectors use an RPN pretrained on base categories to get region proposals. ‡ denotes using mask annotations. † denotes mask AP. ∇ denotes using learnable prompts instead of template prompts. ★ denotes that RegionCLIP use extra pretraining process of 600k iter on CC3M dataset with batch size of 96.

Model	backbone	pretrained CLIP	epochs	external dataset	AP _r	AP _c	AP _f	AP
CLIP on cropped regions‡ [9]	R50-FPN	ViT-B/32	0		19.5	19.7	17.0	18.6
ViLD‡ [9]	R50-FPN	ViT-B/32	384		16.3	21.2	31.6	24.4
RegionCLIP [38]	CLIP R50-C4	RN50	12★	CC3M	17.1	27.4	34.0	28.2
Detic†† [41]	R50-FPN	ViT-B/32	384	ImageNet-21K	17.8	<u>26.3</u>	31.6	<u>26.8</u>
PromptDet∇† [7]	R50-FPN	ViT-B/32	6+12	LAION-novel	<u>19.0</u>	18.5	25.8	21.4
GridCLIP-R50	CLIP R50-FPN	ViT-B/32	24		15.0	22.7	32.5	25.2
GridCLIP-R50-RN	CLIP R50-FPN	RN50x64	24		13.7	23.3	<u>32.6</u>	25.3

Table 2. The training and test time on LVIS v1.0 and the model size comparisons of ViLD and GridCLIP. The resource usage of ViLD is measured based on the implementation of DetPro [5].

Model	Parameters for Inference (M)	Epoch	Training Cost / Epoch (Per-GPU-Hour)	Total Training Cost (Per-GPU-Hour)	FPS
ViLD	60.5	384	7.98	3064	3.3
GridCLIP-R50	56.4	24	2.94	70	19.5
GridCLIP-R50-RN	56.4	24	3.66	88	19.5

Table 3. Generalization ability of LVIS-trained detectors to PASCAL VOC 2007 test set and COCO validation set.

Model	PASCAL VOC		COCO		
	AP ₅₀	AP ₇₅	AP	AP ₅₀	AP ₇₅
ViLD	72.2	56.7	36.6	55.6	39.8
DetPro	74.6	57.9	34.9	53.8	37.4
GridCLIP-R50	70.9	55.4	34.7	52.2	37.1
GridCLIP-R50-RN	71.6	55.7	34.4	51.8	36.6

has a worse generalization ability to novel categories compared to the ViT-B/32 one, with lower AP_r while higher AP_c and AP_f. We further observe the obvious gap between the base and novel categories in GridCLIP, and try to understand and explain the gap based on the analysis from another one-stage detector HierKD [20]. In ViLD, both the novel and base categories use the region-level alignment. In GridCLIP, whilst novel categories use the more coarse-grained image-level alignment, the base categories in GridCLIP use *both* the more fine-grained grid-level alignment and the image-level alignment. This makes the gap between base and novel categories larger than that of ViLD. To verify this, we can replace image-level alignment with region-level alignment similar to ViLD to further improve AP_r, which however may require more training time as other two-stage detectors do. We leave it for future research.

Resources Comparison. We compare GridCLIP with ViLD on training and test time, as well as the model size. ViLD is originally trained on TPUv3 with a batch size of 256. For fair comparison and due to resource limitation, we train both ViLD and GridCLIP with a batch size of 16 on 2 A100 GPUs. We train ViLD using the implementation of DetPro [5]. Moreover, ViLD takes 1 day on 8 V100 GPUs to pre-compute the CLIP image embedding of regions to accelerate training. GridCLIP does not require this. In Ta-

ble 2, we show that with comparable model size, GridCLIP-R50 is approximately $43\times$ and $5\times$ faster than ViLD in training and test respectively. Such significant advantages remain when GridCLIP-R50-RN using RN50 \times 64 ($3\times$ larger in both input and parameters) for image-level alignment, with $34\times$ faster in training time than that of ViLD. This validates clearly the compute efficiency of the one-stage GridCLIP.

Transfer to Other Datasets. To further explore the generalizability of GridCLIP, we follow ViLD [9] and evaluate the LVIS-trained GridCLIP on both the PASCAL VOC 2007 test set [6] and the COCO validation set [18] by directly replacing the categories without any finetuning. Note that there are overlaps of both category and image between LVIS and COCO (as well as PASCAL VOC). The IOU threshold of NMS is 0.6. On PASCAL VOC, we observe that the gap between GridCLIP-R50 and ViLD is 1.2 to 1.3 AP, and GridCLIP-R50-RN is comparable with ViLD on PASCAL VOC with no more than 1 AP difference. Although the gap on COCO is still obvious with 2.2 AP falling behind but is comparable to that of DetPro which uses learn prompts based on ViLD. Therefore, in the generalization ability, GridCLIP performs quite close to its two-stage counterparts.

4.3. Ablation Studies

We verify the effectiveness of grid-level and image-level alignment for undersampled categories for both close-set detection (Table 4) and open-set detection (Table 5). We follow the same settings in Sec. 4.2 except that multi-scaling training and random cropping augmentation are not used here. Among the experiments, “wo align” denotes using the original design of FCOS only with different backbones

Table 4. Comparison of different backbones and alignment methods on LVIS v1.0 [10] with close-set settings. The top section compares supervised (ImageNet [3]) and unsupervised (SwAV [1]) pretrained visual models with CLIP as unsupervised visual-language pretrained model. The bottom section compares different alignment methods based on the ResNet50 version of pretrained CLIP image encoder. “GridCLIP-R50*” uses the CLIP ResNet50 without the MHSA layer, while “GridCLIP-R50” uses the whole image encoder of CLIP ResNet50.

Method	Backbone	Grid-level Alignment	Image-level Alignment	AP_c	AP_f	AP
ImageNet-R50 w/o align	ImageNet R50-FPN	-	-	14.6	26.2	16.6
SwAV-R50 w/o align	SwAV R50-FPN	-	-	19.5	29.2	20.0
GridCLIP-R50* w/o align	CLIP R50-FPN woMHSA	-	-	20.2	30.3	20.7
GridCLIP-R50 w/o align	CLIP R50-FPN			19.4	29.7	20.1
GridCLIP-R50 w grid-align	CLIP R50-FPN	✓		21.7	30.0	21.2
GridCLIP-R50 w image-align	CLIP R50-FPN		✓	19.4	<u>30.1</u>	20.2
GridCLIP-R50	CLIP R50-FPN	✓	✓	<u>21.2</u>	30.0	<u>21.0</u>

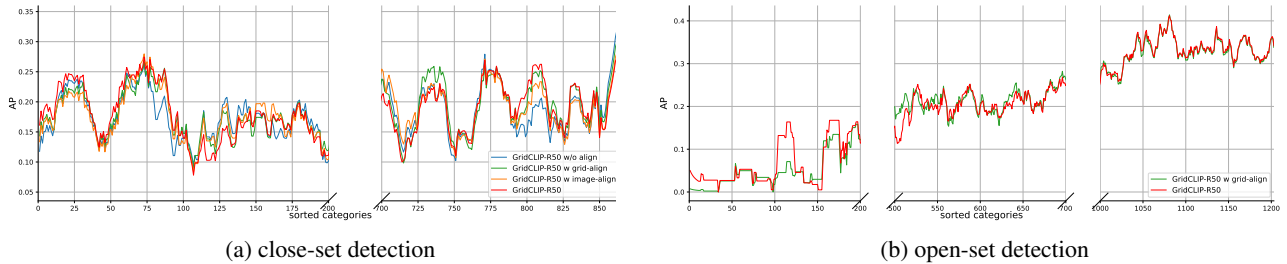


Figure 3. The AP on LVIS v1.0 over categories sorted by frequency in ascending order. (a) uses on the close-set setting, only containing 461 “common” categories and 405 “frequent” categories. (b) uses the open-set setting, containing containing 337 “rare” categories, 461 “common” categories and 405 “frequent” categories. The value is smoothed using moving average with window [-10,10].

Table 5. The effect of image-level alignment on LVIS v1.0 [10] with open-set settings.

Model	AP_r	AP_c	AP_f	AP
GridCLIP-R50 w grid-align	10.1	21.0	29.6	22.5
GridCLIP-R50	12.7	20.6	29.7	22.8

that feed different image features to the FPN. “w grid-align” and “w image-align” denote only using grid-level or image-level alignment respectively.

Close-set Detection. We first evaluate other visual pretrained models as the backbone to compare to the vision-language pretrained model CLIP, including the ImageNet [3] pretrained ResNet50 on the classification task and self-supervised pretrained ResNet50 using visual-only SSL method SwAV [1] pretrained on large-scale unlabeled images. By comparing the methods using different pretrained ResNet50 without any alignment (the top section of Table 4), we notice that using the CLIP pretrained ResNet50 can bring notable improvements compared to the ImageNet and SwAV pretrained ones, with the similar architecture, which indicates the superiority of the vision-language pretrained model CLIP than other visual pretrained models in generalizing better image embeddings for detection.

On the bottom section of Table 4, we introduce the MHSA layer whose output is aligned to the CLIP text encoder in the original training of CLIP. Therefore, the MHSA layer provides both grid-level and image-level features for

CLIP-based alignment. We first observe that introducing the MHSA layer without any alignment drops the overall performance by 0.7 AP, while using both alignments can improve the performance in the infrequent common categories by 1.3 AP and preserves the performance in frequent categories. Among the experiments that use the MHSA layer, we find that applying grid-level alignment can significantly improve the common categories by 2.3 AP, while using image-level alignment seems limited on the metrics AP_c and AP_f . Using both alignments can bring 1.8 AP_c and 0.3 AP_f improvements which are lower than the one using only grid-level alignment. We further explore the reasons behind that. We find that the metric of AP_c and AP_f are too coarse-grained for distinguishing categories with different frequencies. So we further observe the performance in a more fine-grained way by the plot of AP over categories with different sample numbers (Figure 3). As shown in subfigure (a), in the 200 most infrequent categories, the improvement of applying one alignment is not stable, where the AP can be notably higher than “GridCLIP-R50 w/o align” in some categories while obviously worse in other categories. By applying both alignments, “GridCLIP-R50” primarily ranks top in the 100 most infrequent categories, while its superiority is not obvious in frequent categories. Therefore, we can conclude that using both alignments benefits the under-sampled categories in close-set detection.

Open-set Detection. Since only models with grid-level

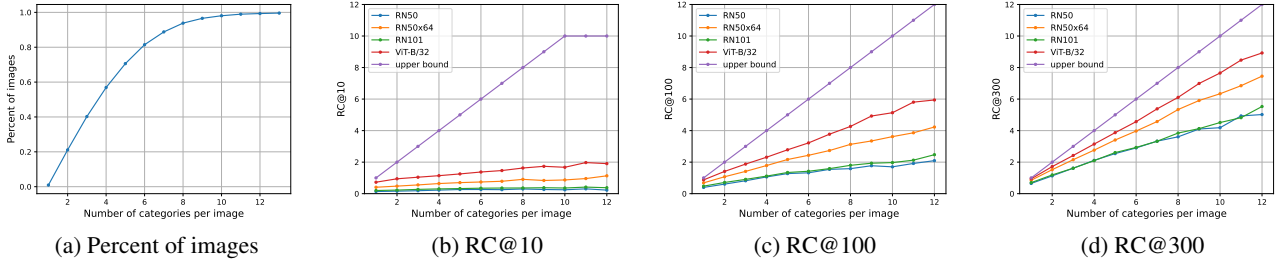


Figure 4. (a) shows the percent of images containing different numbers of categories in an image on LVIS v1.0 validation set. (b), (c) and (d) are the recall of top k ($k=10, 100, 300$) predictions of different CLIP pretrained versions, using the image-level representation from the corresponding CLIP image encoder.

alignment can be extended for open-set detection by extending the categories embedding list with novel categories and using the list match with the grid-level image embeddings, we compare two models from Table 4. As shown in Table 5, image-level alignment improves novel categories by 2.6 AP_r, while preserving the performance on base categories. Also, as shown in Figure 3 (b), the performance rises over categories as their training sample number increases, which verifies that undersampled categories suffer from long-tail distribution. In the 200 most infrequent categories which are novel (also rare) categories, “GridCLIP-R50” outperforms “GridCLIP-R50 w grid-align” significantly, which indicates the effectiveness of image-level alignment on novel categories. Therefore, it is verified the alignment of image-level representations also helps learn generalizable grid-level representations of undersampled categories.

In summary, grid-level alignment improves the performance notably on undersampled categories in close-set detection and allows the detector to be extended for open-set detection, while image-level alignment obviously benefits the novel categories in open-set detection. Using both alignments enables a one-stage detector to detect novel categories and mitigate the deterioration of undersampled categories in long-tail datasets.

4.4. Further Analysis: Evaluating CLIP Image-Level Representation for Object Detection

We analyse how accurately the multiple categories in an image can be represented by the original CLIP image encoder. This substantially affects the performance of a one-stage detector built upon the CLIP image-level representation to detect multiple categories at the same time, which indicates how much image-level alignment can benefit GridCLIP. We evaluate several pretrained versions of CLIP on LVIS v1.0 validation set, including the refined ResNet [11] (RN50, RN101, RN50x64) and those with the Transformer architecture [4] (ViT-B/32). Specifically, We calculate the recall of categories by using the original CLIP image-level representation to match the text representation of each cat-

egory (Figure 4).

For RC@10, all models perform poorly with no more than 2 recalls. While for RC@100, we find that ViT-B/32 can recall 50% of the categories and RN50x64 can recall more than 30% of the categories. In comparison, the other ResNet-based models perform poorly that reach less than 20% recall rate. Furthermore, for RC@300, nearly 75% of the categories in an image are captured by ViT-B/32, and RN50x64 reaches about 60% recall rate. Given that the maximum detection number for LVIS v1.0 in OVID is usually set to 300 (objects), ViT-B/32 can at most help detect 75% of the objects if all the objects have different categories and 50% if every 3 of the objects share the same category. This provides substantial knowledge of categories to help the detector build the representation for multiple object detection. Therefore, the CLIP image encoder is able to capture multiple categories in an image at the same time with relatively high accuracy and provide substantial knowledge of categories for the detector during image-level alignment.

5. Conclusion

In this work, we introduce a one-stage detector GridCLIP, which exploits the CLIP representation space to supplement the knowledge on undersampled categories in downstream detection datasets. GridCLIP optimizes generalizable knowledge from the CLIP pretrained representation to more fine-grained localized mapping, by simultaneously learning a localized grid-level CLIP mapping to base categories (Grid-level Alignment) and a holistic image-level knowledge distillation to base and novel categories in a target object detection domain (Image-level Alignment). In our experiments, we verify that GridCLIP suffers less from long-tail distributions with the help of both grid-level and image-level alignments, reaching comparable performance on the LVIS v1.0 benchmark with higher training and inference speed.

References

- [1] Mathilde Caron, Ishan Misra, Julien Mairal, Priya Goyal, Piotr Bojanowski, and Armand Joulin. Unsupervised learning of visual features by contrasting cluster assignments. *Advances in Neural Information Processing Systems*, 33:9912–9924, 2020.
- [2] Kai Chen, Jiaqi Wang, Jiangmiao Pang, Yuhang Cao, Yu Xiong, Xiaoxiao Li, Shuyang Sun, Wansen Feng, Ziwei Liu, Jiarui Xu, et al. Mmdetection: Open mmlab detection toolbox and benchmark. *arXiv preprint arXiv:1906.07155*, 2019.
- [3] Jia Deng, Wei Dong, Richard Socher, Li-Jia Li, Kai Li, and Li Fei-Fei. Imagenet: A large-scale hierarchical image database. In *2009 IEEE conference on computer vision and pattern recognition*, pages 248–255. Ieee, 2009.
- [4] Alexey Dosovitskiy, Lucas Beyer, Alexander Kolesnikov, Dirk Weissenborn, Xiaohua Zhai, Thomas Unterthiner, Mostafa Dehghani, Matthias Minderer, Georg Heigold, Sylvain Gelly, Jakob Uszkoreit, and Neil Houlsby. An image is worth 16x16 words: Transformers for image recognition at scale. In *9th International Conference on Learning Representations, ICLR 2021, Virtual Event, Austria, May 3-7, 2021*. OpenReview.net, 2021.
- [5] Yu Du, Fangyun Wei, Zihe Zhang, Miaojing Shi, Yue Gao, and Guoqi Li. Learning to prompt for open-vocabulary object detection with vision-language model. In *Proceedings of the IEEE/CVF Conference on Computer Vision and Pattern Recognition*, pages 14084–14093, 2022.
- [6] Mark Everingham, Luc Van Gool, Christopher KI Williams, John Winn, and Andrew Zisserman. The pascal visual object classes (voc) challenge. *International journal of computer vision*, 88(2):303–338, 2010.
- [7] Chengjian Feng, Yujie Zhong, Zequn Jie, Xiangxiang Chu, Haibing Ren, Xiaolin Wei, Weidi Xie, and Lin Ma. Prompt-det: Expand your detector vocabulary with uncured images. *arXiv preprint arXiv:2203.16513*, 2022.
- [8] Mingfei Gao, Chen Xing, Juan Carlos Niebles, Junnan Li, Ran Xu, Wenhao Liu, and Caiming Xiong. Towards open vocabulary object detection without human-provided bounding boxes. *arXiv preprint arXiv:2111.09452*, 2021.
- [9] Xiuye Gu, Tsung-Yi Lin, Weicheng Kuo, and Yin Cui. Open-vocabulary object detection via vision and language knowledge distillation. In *The Tenth International Conference on Learning Representations, ICLR 2022, Virtual Event, April 25-29, 2022*. OpenReview.net, 2022.
- [10] Agrim Gupta, Piotr Dollar, and Ross Girshick. Lvis: A dataset for large vocabulary instance segmentation. In *Proceedings of the IEEE/CVF conference on computer vision and pattern recognition*, pages 5356–5364, 2019.
- [11] Kaiming He, Xiangyu Zhang, Shaoqing Ren, and Jian Sun. Deep residual learning for image recognition. In *Proceedings of the IEEE conference on computer vision and pattern recognition*, pages 770–778, 2016.
- [12] Tony Huang, Jack Chu, and Fangyun Wei. Unsupervised prompt learning for vision-language models. *arXiv preprint arXiv:2204.03649*, 2022.
- [13] Chao Jia, Yinfei Yang, Ye Xia, Yi-Ting Chen, Zarana Parekh, Hieu Pham, Quoc Le, Yun-Hsuan Sung, Zhen Li, and Tom Duerig. Scaling up visual and vision-language representation learning with noisy text supervision. In *International Conference on Machine Learning*, pages 4904–4916. PMLR, 2021.
- [14] Weicheng Kuo, Yin Cui, Xiuye Gu, AJ Piergiovanni, and Anelia Angelova. F-vm: Open-vocabulary object detection upon frozen vision and language models. *arXiv preprint arXiv:2209.15639*, 2022.
- [15] Junnan Li, Ramprasaath Selvaraju, Akhilesh Gotmare, Shafiq Joty, Caiming Xiong, and Steven Chu Hong Hoi. Align before fuse: Vision and language representation learning with momentum distillation. *Advances in neural information processing systems*, 34:9694–9705, 2021.
- [16] Liunian Harold Li, Pengchuan Zhang, Haotian Zhang, Jianwei Yang, Chunyuan Li, Yiwu Zhong, Lijuan Wang, Lu Yuan, Lei Zhang, Jenq-Neng Hwang, et al. Grounded language-image pre-training. In *Proceedings of the IEEE/CVF Conference on Computer Vision and Pattern Recognition*, pages 10965–10975, 2022.
- [17] Tsung-Yi Lin, Priya Goyal, Ross Girshick, Kaiming He, and Piotr Dollár. Focal loss for dense object detection. In *Proceedings of the IEEE international conference on computer vision*, pages 2980–2988, 2017.
- [18] Tsung-Yi Lin, Michael Maire, Serge Belongie, James Hays, Pietro Perona, Deva Ramanan, Piotr Dollár, and C Lawrence Zitnick. Microsoft coco: Common objects in context. In *European conference on computer vision*, pages 740–755. Springer, 2014.
- [19] Timo Lüddecke and Alexander S Ecker. Prompt-based multi-modal image segmentation. *arXiv preprint arXiv:2112.10003*, 2021.
- [20] Zongyang Ma, Guan Luo, Jin Gao, Liang Li, Yuxin Chen, Shaoru Wang, Congxuan Zhang, and Weiming Hu. Open-vocabulary one-stage detection with hierarchical visual-language knowledge distillation. In *Proceedings of the IEEE/CVF Conference on Computer Vision and Pattern Recognition*, pages 14074–14083, 2022.
- [21] Alec Radford, Jong Wook Kim, Chris Hallacy, Aditya Ramesh, Gabriel Goh, Sandhini Agarwal, Girish Sastry, Amanda Askell, Pamela Mishkin, Jack Clark, et al. Learning transferable visual models from natural language supervision. In *International Conference on Machine Learning*, pages 8748–8763. PMLR, 2021.
- [22] Yongming Rao, Wenliang Zhao, Guangyi Chen, Yansong Tang, Zheng Zhu, Guan Huang, Jie Zhou, and Jiwen Lu. Denseclip: Language-guided dense prediction with context-aware prompting. In *IEEE/CVF Conference on Computer Vision and Pattern Recognition, CVPR 2022, New Orleans, LA, USA, June 18-24, 2022*, pages 18061–18070. IEEE, 2022.
- [23] Shaoqing Ren, Kaiming He, Ross Girshick, and Jian Sun. Faster r-cnn: Towards real-time object detection with region proposal networks. *Advances in neural information processing systems*, 28, 2015.
- [24] Alexander I Saichev, Yannick Malevergne, and Didier Sornette. *Theory of Zipf’s law and beyond*, volume 632. Springer Science & Business Media, 2009.
- [25] Piyush Sharma, Nan Ding, Sebastian Goodman, and Radu Soricut. Conceptual captions: A cleaned, hypemymed, im-

- age alt-text dataset for automatic image captioning. In *Proceedings of the 56th Annual Meeting of the Association for Computational Linguistics (Volume 1: Long Papers)*, pages 2556–2565, 2018.
- [26] Amanpreet Singh, Ronghang Hu, Vedanuj Goswami, Guillaume Couairon, Wojciech Galuba, Marcus Rohrbach, and Douwe Kiela. FLAVA: A foundational language and vision alignment model. In *IEEE/CVF Conference on Computer Vision and Pattern Recognition, CVPR 2022, New Orleans, LA, USA, June 18-24, 2022*, pages 15617–15629. IEEE, 2022.
 - [27] Peize Sun, Rufeng Zhang, Yi Jiang, Tao Kong, Chenfeng Xu, Wei Zhan, Masayoshi Tomizuka, Lei Li, Zehuan Yuan, Changhu Wang, et al. Sparse r-cnn: End-to-end object detection with learnable proposals. In *Proceedings of the IEEE/CVF conference on computer vision and pattern recognition*, pages 14454–14463, 2021.
 - [28] Zhi Tian, Chunhua Shen, Hao Chen, and Tong He. Fcos: Fully convolutional one-stage object detection. In *Proceedings of the IEEE/CVF international conference on computer vision*, pages 9627–9636, 2019.
 - [29] Ashish Vaswani, Noam Shazeer, Niki Parmar, Jakob Uszkoreit, Llion Jones, Aidan N Gomez, Łukasz Kaiser, and Illia Polosukhin. Attention is all you need. *Advances in neural information processing systems*, 30, 2017.
 - [30] Fangyun Wei, Yue Gao, Zhirong Wu, Han Hu, and Stephen Lin. Aligning pretraining for detection via object-level contrastive learning. *Advances in Neural Information Processing Systems*, 34, 2021.
 - [31] Johnathan Xie and Shuai Zheng. Zsd-yolo: Zero-shot yolo detection using vision-language knowledge distillation. *arXiv preprint arXiv:2109.12066*, 2021.
 - [32] Ceyuan Yang, Zhirong Wu, Bolei Zhou, and Stephen Lin. Instance localization for self-supervised detection pretraining. In *Proceedings of the IEEE/CVF Conference on Computer Vision and Pattern Recognition*, pages 3987–3996, 2021.
 - [33] Lu Yuan, Dongdong Chen, Yi-Ling Chen, Noel Codella, Xiyang Dai, Jianfeng Gao, Houdong Hu, Xuedong Huang, Boxin Li, Chunyuan Li, et al. Florence: A new foundation model for computer vision. *arXiv preprint arXiv:2111.11432*, 2021.
 - [34] Alireza Zareian, Kevin Dela Rosa, Derek Hao Hu, and Shih-Fu Chang. Open-vocabulary object detection using captions. In *Proceedings of the IEEE/CVF Conference on Computer Vision and Pattern Recognition*, pages 14393–14402, 2021.
 - [35] Haotian Zhang, Pengchuan Zhang, Xiaowei Hu, Yen-Chun Chen, Liunian Harold Li, Xiyang Dai, Lijuan Wang, Lu Yuan, Jenq-Neng Hwang, and Jianfeng Gao. GlipV2: Unifying localization and vision-language understanding. In *Advances in Neural Information Processing Systems*, 2022.
 - [36] Pengchuan Zhang, Xiujun Li, Xiaowei Hu, Jianwei Yang, Lei Zhang, Lijuan Wang, Yejin Choi, and Jianfeng Gao. Vinvl: Revisiting visual representations in vision-language models. In *Proceedings of the IEEE/CVF Conference on Computer Vision and Pattern Recognition*, pages 5579–5588, 2021.
 - [37] Shifeng Zhang, Cheng Chi, Yongqiang Yao, Zhen Lei, and Stan Z. Li. Bridging the gap between anchor-based and anchor-free detection via adaptive training sample selection. In *Proceedings of the IEEE/CVF Conference on Computer Vision and Pattern Recognition (CVPR)*, June 2020.
 - [38] Yiwu Zhong, Jianwei Yang, Pengchuan Zhang, Chunyuan Li, Noel Codella, Liunian Harold Li, Luowei Zhou, Xiyang Dai, Lu Yuan, Yin Li, and Jianfeng Gao. Regionclip: Region-based language-image pretraining. In *IEEE/CVF Conference on Computer Vision and Pattern Recognition, CVPR 2022, New Orleans, LA, USA, June 18-24, 2022*, pages 16772–16782. IEEE, 2022.
 - [39] Chong Zhou, Chen Change Loy, and Bo Dai. Denseclip: Extract free dense labels from clip. *arXiv preprint arXiv:2112.01071*, 2021.
 - [40] Kaiyang Zhou, Jingkang Yang, Chen Change Loy, and Ziwei Liu. Learning to prompt for vision-language models. *Int. J. Comput. Vis.*, 130(9):2337–2348, 2022.
 - [41] Xingyi Zhou, Rohit Girdhar, Armand Joulin, Phillip Krähenbühl, and Ishan Misra. Detecting twenty-thousand classes using image-level supervision. *arXiv preprint arXiv:2201.02605*, 2022.